Momentum-dependent dielectric functions of oriented *trans*-polyacetylene

J. Fink

*Institut für Nukleare Festkörperphysik, Kernforschungszentrum Karlsruhe G.m.b.H., Postfach 3640,
D-7500 Karlsruhe 1, Federal Republic of Germany*

G. Leising

Institut für Festkörperphysik, Technische Universität Graz, Petersgasse 16, A-8010 Graz, Austria
(Received 14 April 1986)

The momentum-dependent dielectric functions parallel and perpendicular to the chain axis of highly oriented nonfibrous crystalline *trans*-polyacetylene were determined by electron-energy-loss spectroscopy in the energy and momentum range 0.2—30 eV and 0.05—1.2 Å^{-1}, respectively. Information on the electronic structure of π and σ bands as well as on collective excitations was obtained. In particular, a total width of the π bands of $4t_0 = 12.8 \pm 0.5$ eV is derived. In addition, from the sum rule for π-electron excitations the ratio of the correlation energy U to the total width of the π bands $U/4t_0 \sim 0.7$ is estimated. Most of the experimental results can be explained in a single-particle picture. The momentum-independent absorption edge is most likely explained by excitonic transitions.

I. INTRODUCTION

The recent interest in the electronic structure of conjugated polymers has been stimulated by their enormous changes in conductivity upon doping. In particular, polyacetylene, $(CH)_x$, has been the focus of most of the experimental and theoretical work.[1] Therefore, the understanding of the electronic structure of undoped $(CH)_x$ is the basis for similar studies of doped $(CH)_x$. In addition, the *trans*conformation of $(CH)_x$ is the prototype of infinite polyenes, the electronic structure of which has been a subject of controversy for decades.[2-10] In particular, the nature of the fundamental absorption edge is still under discussion. The question is, whether the single particle models are the appropriate theoretical framework to describe elementary excitations in these quasi-one-dimensional semiconductors or whether electron correlations must be considered.

To clarify this question and to get more information on the electronic structure of undoped *trans*-polyacetylene, we measured the momentum-dependent dielectric functions by electron-energy-loss spectroscopy (ELS) on highly oriented nonfibrous crystalline $(CH)_x$. We have obtained information on interband transitions and plasmons in a large energy range (0.2—30 eV) and a large momentum transfer range (0.05—1.2 Å^{-1}) with polarization parallel and perpendicular to the chain axis. We compare our results with band-structure calculations[11,12] and with calculations of the dielectric functions[13-16] for *trans*-$(CH)_x$. In addition, we analyzed our data by comparing them to simple calculations of the momentum-dependent joint density of states in a tight-binding scheme.

This work is an extension of previous studies on fibrous *trans* polyacetylene by optical spectroscopy on less well-oriented samples,[13,17] by synchrotron radiation on nonoriented samples,[18] and by ELS on nonoriented samples.[19,20]

II. EXPERIMENTAL

Fully oriented nonfibrous polyacetylene films with a thickness of about 2000 Å were prepared by a route[21] which is based on the synthesis of Edwards and Feast.[22] The precursor polymer poly-7,8-bis-(trifluoromethyl)-tricyclo-[4.2.2.0]-deka-3,7,9-triene [poly-(BTFM-TCDT)] is produced by a ring opening metathetical polymerization of the monomer BTFM-TCDT in solution with the catalyst system WCl_6 and $(CH_3)_4Sn$. Films were cast from solution of the precursor polymer and were converted to oriented polyacetylene by applying an appropriate stress at temperatures up to 120 °C. During the conversion, an elongation of the polymer film by a factor of 20 and a simultaneous alignment of the polymer chains take place. All reactions and also the transfer to the ELS spectrometer were carried out under high vacuum or under pure argon atmosphere. Films prepared in this way are 100% *trans*-$(CH)_x$ as evidenced from the lack of the cis-C-H out-of-plane vibration at 740 cm^{-1}. The material exhibits a compact, nonfibrous dense morphology and smooth surfaces as found by scanning electron microscopy. The density is about 1.1 g/cm^3 which is close to the theoretical x-ray density of 1.2 g/cm^3. The degree of the orientation of the chain axis was obtained from the rocking curve of the (002) reflection, measured in the ELS spectrometer with zero energy loss. The intensity of the (002) reflection was recorded in transmission as a function of the angle between a certain direction in the polymer film and the scattering plane. The full width at half maximum of this rocking curve was taken as a quantitative measure of the degree of the orientation of the chains. Typical values were better than 5°, indicating highly oriented films.

The transmission ELS measurements and elastic electron diffraction measurements were performed using a spectrometer[23] with a primary electron energy of 170 keV and an energy and momentum resolution chosen to be

0.15 eV and 0.03 Å^{-1}, respectively. The current density on the sample was less than 10^{-6} A/cm^2. Therefore, measurements on the same sample could be carried out for several days before observing changes in the spectra due to radiation damage. For doses of about 1 C/cm^2, a broadening of the π plasmon and of the $\sigma \rightarrow \sigma^*$ transitions as well as of the diffraction peaks was observed. Up to now, we have not studied systematically the radiation damage in *trans*-(CH)$_x$. In almost all measurements the sample was kept at 80 K. To get information on the contributions from phonon-assisted indirect transitions, some measurements were performed at higher temperatures.

In order to evaluate the dielectric functions from the loss function Im($-1/\epsilon$), we closely followed the procedure described by Daniels *et al.*[24] From the loss spectrum taken from -2 to 48 eV, the elastic line was removed and contributions from double scattering were subtracted. Furthermore, the spectrum was deconvoluted to account for finite momentum resolution of the spectrometer. The loss function was then normalized so as to reproduce the value of the real part of the dielectric function ϵ_1 at low energies, which can be deduced for zero momentum transfer from the refractive index $n = \sqrt{\epsilon_1}$. These refractive indexes parallel and perpendicular to the chain axis were obtained by infrared measurements ($E = 0.25$ eV) of the Fabry-Perot resonance periods. The values $n^{\parallel} = 3.25$ and $n^{\perp} = 1.33$ derived[25] for thin films ($d \leq 1$ μm) are slightly different from values given in a previous publication,[26] since experimental improvement in the preparation route results in samples with less variation in thickness and thus in better pronounced multiple beam interferences. For the analysis of spectra taken at higher momentum transfer, theoretical models for the momentum dependence of the refractive index have to be used.

From the normalized loss function Im($-1/\epsilon$), the real part of $1/\epsilon$ can be deduced from a standard Kramers-Kronig analysis. Once the real and imaginary parts of $1/\epsilon$ are known, the dielectric functions ϵ_1 and ϵ_2, the optical joint density of states, the reflectivity, and the absorption constant can be calculated.

III. RESULTS

In the case of an anisotropic crystal, the scattering cross section for high-energy electrons is proportional to the energy-loss functions[27] Im($-1/\mathbf{q}\cdot\hat{\epsilon}\cdot\mathbf{q}$) where $\hat{\epsilon}(\mathbf{q},\omega)$ is the dielectric tensor. For a uniaxial crystal, this loss function can be written as Im($-1/(\epsilon^{\parallel}\cos^2\theta + \epsilon^{\perp}\sin^2\theta)$) where $\epsilon^{\parallel}$ and $\epsilon^{\perp}$ are the principal components of $\hat{\epsilon}$ parallel and perpendicular to the symmetry axis and θ is the angle between the symmetry axis and the momentum transfer. Therefore, for well-oriented samples, a separation of the loss function according to the two directions is possible.

In Fig. 1 we show typical loss spectra of *trans*-polyacetylene for various angles θ between the chain axis and the momentum transfer. A small momentum transfer $q = 0.1$ Å^{-1} was chosen in order to avoid contributions from surface losses and radiation losses.[24] The loss functions, derived for $\theta = 0°$ and 90° as described in the preceding section are shown in Fig. 2. For $\mathbf{q}$ parallel to the chain axis, the most pronounced structures are the $\sigma + \pi$
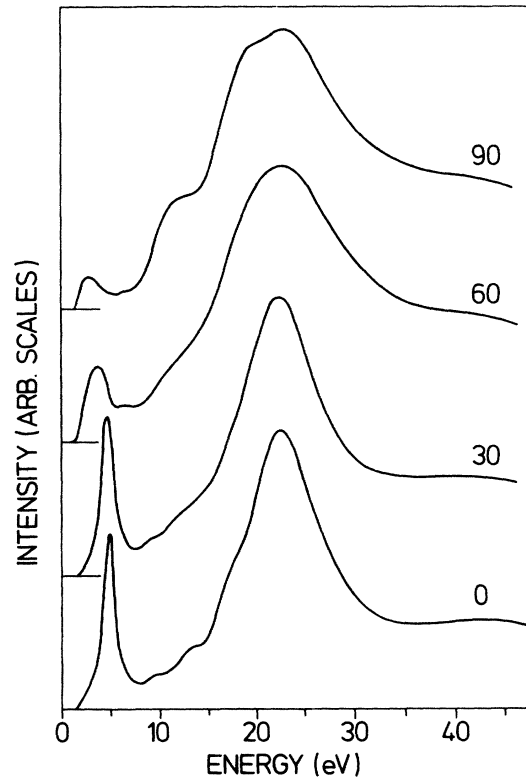

FIG. 1. Electron-energy-loss spectra of highly oriented polyacetylene as a function of the angle between the momentum transfer and the chain axis.

electron plasmon at 22.5 eV and the π-electron plasmon at 4.9 eV. These structures were already identified by Ritsko *et al.*[19] in an ELS study of nonoriented polyacetylene. In addition, we observe several shoulders between the π and the $\sigma + \pi$ plasmon. The spectrum clearly shows a threshold at 1.4 eV. Below this threshold, the intensity of the losses is less than 5×10^{-3} of that of the π plasmon. By a Kramers-Kronig analysis, the real and the imaginary part of the dielectric functions $\epsilon_1^{\parallel}$ and $\epsilon_2^{\parallel}$ were derived. These functions are also shown in Fig. 2. There is a strong oscillator near 2 eV corresponding to a $\pi \rightarrow \pi^*$ transition. At higher energy, additional oscillators due to $\sigma \rightarrow \sigma^*$ transitions are observed. With increasing angle θ, the π plasmon in the loss function moves to lower energies. This can be well explained by calculating the θ-dependent loss function for the given $\epsilon_1^{\parallel}$ and $\epsilon_2^{\parallel}$ and with $\epsilon_2^{\perp} \ll \epsilon_2^{\parallel}$ and $\epsilon_1^{\perp} = 1.77$. For $\mathbf{q}$ perpendicular to the chain axis ($\theta = 90°$) a considerable flattening and a shift of the π plasmon and the $\sigma + \pi$ plasmon is observed. Similar changes of the π and $\pi + \sigma$ plasmon were reported for graphite by Chen and Silcox.[28] The residual maximum of the loss function near 2 eV may be not only caused by the dielectric function $\epsilon^{\perp}$ but also by contributions of $\epsilon^{\parallel}$ due to finite momentum resolution or to misaligned chains. An estimate of the magnitude of these contributions shows that it is small and therefore causes only minor errors in Im($-1/\epsilon^{\perp}$). From the Kramers-Kronig analysis of the loss function Im($-1/\epsilon^{\perp}$) we have derived the dielectric
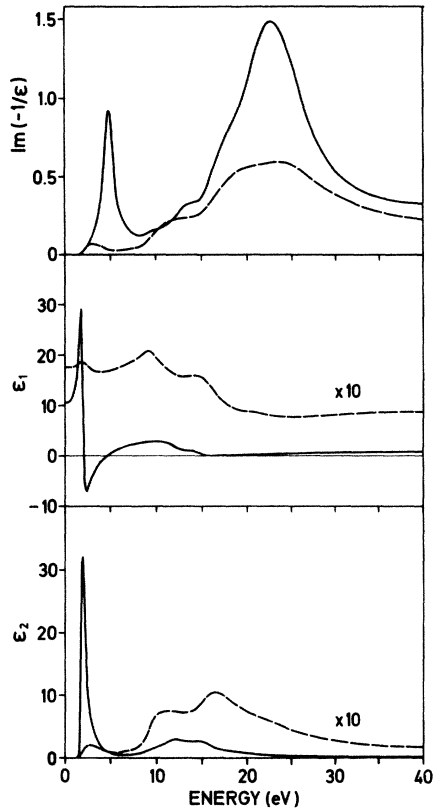
FIG. 2. Loss function $Im(-1/\epsilon)$, real and imaginary part of the dielectric function ϵ_1 and ϵ_2 for highly oriented polyacetylene. Momentum transfer was $q=0.1$ Å^{-1}. Solid line: q parallel to the chain axis. Dashed line: q perpendicular to the chain axis.

FIG. 3. Momentum dependence of the loss function for q (in Å^{-1}) parallel to the chain axis. A linear dispersion of the π plasmon and a strong decay near $q=1$ Å^{-1} are observed.

functions $\epsilon_1^\perp$ and $\epsilon_2^\perp$, also shown in Fig. 2. A strong anisotropy of the $\pi \rightarrow \pi^*$ oscillator is observed in the ϵ_2 functions. At higher energies, other oscillators related to σ bands appear.

In order to obtain more information on the electronic structure of polyacetylene, we have also taken loss spectra at higher momentum transfer. Figure 3 shows the π plasmon as a function of momentum transfer parallel to the chain axis for $q=0.1$ to 1.2 Å^{-1}. The linear dispersion of the π plasmon, already observed by Ritsko et al.[19] in a smaller momentum-transfer range, can clearly be recognized. The spectra also reveal a strong decay of the π plasmon near $q=1.0$ Å^{-1}. The threshold of the loss function shows no dispersion. In all spectra the onset of the loss function is very close to 1.4 eV.

For various momentum transfers $q>0.1$ Å^{-1} we have also performed the Kramers-Kronig analysis of the loss function. For the momentum dependence of the refractive index n, which is needed to obtain the absolute value of the loss function (see previous section), we have used two different theoretical models. For q parallel to the chain axis, we have taken $n(q)$ from the RPA calculations of Drechsler and Bobeth[16] taking into account the slightly smaller $n(0)$ of our samples. For q perpendicular to the
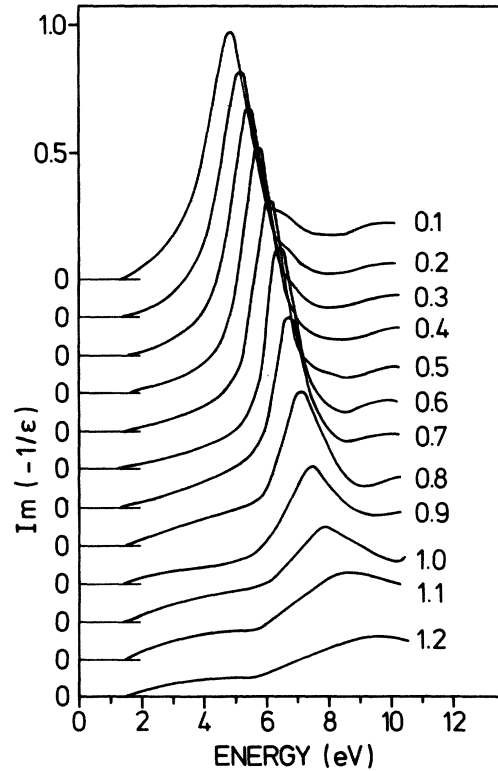
chain axis, we have used the Thomas-Fermi theory of Resta[29] for an isotropic semiconductor, which gives only a weak momentum dependence of the refractive index. From the derived momentum-dependent dielectric functions we show the momentum-dependent optical joint density of states (OJDS) which is defined as

$$J(q,E) = \frac{E\epsilon_2(q,E)}{\frac{1}{2}\pi E_p^2},$$

where E_p is the free electron plasma energy

$$E_p = \hbar \left[\frac{4\pi e^2 N}{mV} \right]^{1/2}.$$

N is the number of valence electrons per unit cell, V is the volume of the unit cell, and m is the free electron mass.

Figure 4(a) shows the OJDS with momentum transfer parallel to the chain axis. The curves show the strong linear dispersion of the $\pi \rightarrow \pi^*$ oscillator for $q \leq 0.7$ Å^{-1}. Also for the oscillators at high energies, a dispersion is observed. For q perpendicular to the chain axis, the momentum-dependent OJDS is shown in Fig. 5. Besides a small change in the energy range 1.4–6 eV, there is no dispersion of the interband transition. The small maximum which appears near 5 eV in the OJDS for higher momentum transfer $(q \geq 0.7$ Å$^{-1})$ originates probably from a double-scattering process due to a quasielastic scattering with momentum transfer q and an excitation of a π plasmon or a surface π plasmon with $q=0$. This as-
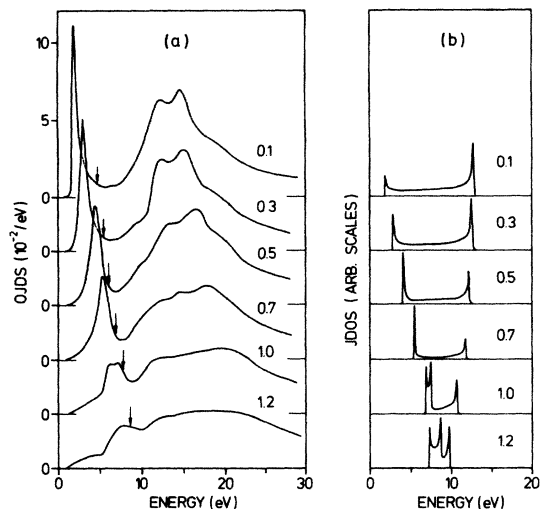
FIG. 4. (a) Momentum dependence of the optical joint density of states (OJDS) for q (in $\mathring{A}^{-1}$) parallel to the chain axis. Curves were derived from a Kramers-Kronig analysis of the loss function. Arrows indicate the position of the π plasmon. (b) Momentum-dependent joint density of states of π bands (q parallel to the chain axis) calculated in a simple tight-binding scheme. Matrix element effects which suppress the higher parts of the joint density are not included in the calculations.

signment is supported by a rough estimate of this intensity using the spectrum for $q=0$ and the momentum dependence of the quasielastic intensity. This type of double scattering which strongly increases at higher momentum transfer, makes measurements at higher momentum transfers more and more difficult. Spectra taken at $q=2$
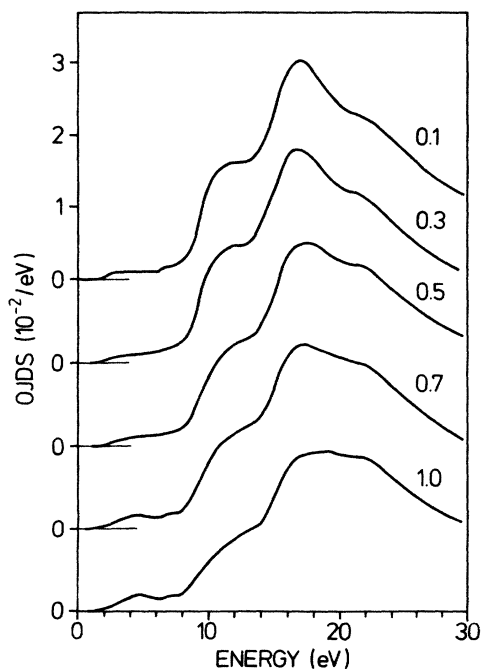

FIG. 5. Momentum dependence of the optical joint density of states (OJDS) for q (in $\mathring{A}^{-1}$) perpendicular to the chain axis. Curves were derived from a Kramers-Kronig analysis of the loss function.

$\mathring{A}^{-1}$ show almost the loss function for zero momentum transfer. Therefore, measurements of the dielectric functions at momentum transfer $q \geq 1.2$ $\mathring{A}^{-1}$ are not feasible with samples of thickness $\cong 2000$ $\mathring{A}$. However, a strong reduction in thickness of these oriented polyacetylene films seems to be very difficult at present.

Finally we mention that measurements of the loss function for $q^{\parallel}=0.1$ and 0.7 $\mathring{A}^{-1}$ at two higher temperatures, i.e., $T=290$ and 390 K show almost no changes compared to the low-temperature results.

IV. DISCUSSION

First, we discuss the dielectric functions measured at small momentum transfer $q=0.1$ $\mathring{A}^{-1}$ which should be close to those dielectric functions derived from optical spectroscopy. The imaginary part of the dielectric function $\epsilon_2^{\parallel}$ (see Fig. 2) shows an onset at 1.4 eV and a maximum at 1.9 eV followed by a continuum of excitations at higher energies. The shape of the spectrum is close to calculations of $\epsilon_2^{\parallel}(0,E)$ in a tight-binding scheme, predicting a square-root singularity.[30] Of course, in the experiment the singularity is broadened due to local field effects, exchange,[15] finite energy resolution, finite chain length, disorder, and interchain coupling. The energy positions of the maxima in $\epsilon_2^{\parallel}$ (1.9 eV), in the $\mathscr{J}^{\parallel}$ (1.95 eV) and in the absorption $\mu^{\parallel}$ (2.3 eV) are slightly higher than values obtained by optical spectroscopy on fibrous low-density Shirakawa material. Fincher et al.[17] report a maximum at 1.8 eV for the optical conductivity, derived from a Kramers-Kronig analysis of reflectivity data and the maximum for the absorption lies near 1.9 eV. These small discrepancies can be explained by the fact that the ELS spectra were taken at a small but finite momentum-transfer value $q=0.1$ $\mathring{A}^{-1}$. The extrapolation to zero momentum transfer for $\epsilon_2^{\parallel}$, $\mathscr{J}^{\parallel}$, and $\mu^{\parallel}$ is not straightforward, as the momentum dependence of the $\pi \rightarrow \pi^*$ oscillator is not clear for small q. From the calculation of the joint density of the π bands, which will be discussed later in detail (see also Refs. 15 and 16), a parabolic q dependence of the energy of the $\pi \rightarrow \pi^*$ oscillator is expected for small momentum transfer. This will result in a decrease of the energy position of the maximum in the $\mathscr{J}^{\parallel}$ by about 0.15 eV to a value of 1.8 eV now in excellent agreement with the results from optical spectroscopy.[17]

Regarding the absolute value of the dielectric function in the energy range of the $\pi \rightarrow \pi^*$ transitions, again differences appear between the present ELS data and optical data on Shirakawa material, which may be caused by the different degree of orientation and by the different density of the material used in optical investigations. The maximum values for the dielectric functions of the π system derived from ELS data are for the optical conductivity $\sigma^{\parallel}=9.5 \times 10^3$ $(\Omega \, cm)^{-1}$, for the absorption $\mu^{\parallel}=8.5 \times 10^5$ cm^{-1}, for the reflectance $R^{\parallel}=0.60$, and $\epsilon_1^{\parallel}=28$, while those obtained by optical spectroscopy for oriented Shirakawa films are,[17] $\sigma^{\parallel}=4 \times 10^3$ $(\Omega \, cm)^{-1}$, $\mu^{\parallel}=3 \times 10^5$ cm^{-1}, $R^{\parallel}=0.48$, and $\epsilon_1^{\parallel}=18.5$. Taking into account a factor of 3 due to the three times higher density of our polyacetylene compared to that used in the optical investigations, the optical absorption is almost the same as that

derived from the ELS data.

Information on the optical effective mass m^* of the π electrons for q parallel to the chain axis can be obtained by using the oscillator strength sum rule:[31]

$$\int_0^{E_c} J(\mathbf{q},E)dE = \frac{n_{eff}}{n}\frac{m}{m^*} ,$$

where n_{eff} is the effective number of electrons per CH group contributing to the optical properties for $E < E_c$, n is the number of valence electrons per CH group, and m is the free electron mass. Taking $E_c \sim 6$ eV, the $\pi \rightarrow \pi^*$ oscillator strength is almost fully exhausted, no contributions from σ electrons are expected, and therefore $n_{eff}/n = \frac{1}{5}$. With these parameters, the evaluation of the sum rule for several spectra taken at $q=0.1$ Å^{-1} yields the average result $m^*/m = 1.7 \pm 0.1$. It is remarkable that the same effective mass was also obtained for higher momentum transfer up to $q \leq 0.7$ Å^{-1}. On the basis of the Su-Schrieffer-Heeger (SSH) Hamiltonian,[30] Baeriswyl et al.[13] have calculated the effective mass $m^* = \pi \hbar^2 / 4 t_0 a^2$, where a is the lattice constant in the chain direction and $4t_0$ is the total width of the π bands. Using $a = 1.2$ Å and $4t_0 = 12.8$ eV as derived from the momentum-dependent measurements, which will be discussed later, we obtain $m^*/m = 1.3$. The deviation from the experimental value $m^*/m = 1.7$ may be caused by electron-electron correlations, not taken into account in the SSH Hamiltonian, as these correlations tend to increase the effective optical mass.[32] According to a calculation of the sum rule in the framework of the one-dimensional Hubbard model the ratio of the correlation energy U divided by $4t_0$ can be calculated from the sum rule.[33] For small $U/4t_0$, the ratio of the single-particle effective mass m^* to the effective mass m_H^* in the Hubbard model is given by $m^*/m_H^* = 1 - 0.21 (U/4t_0)^2$. Using the exact relation for higher $U/4t_0$ as given by Eq. (6) of Ref. 33, we obtain $U/4t_0 = 0.9$. The dimerization, not taken into account in this model, slightly reduces this value. A rough estimate of this reduction[34] on the basis of calculations by Baeriswyl and Maki[35] yields that the present experimental results of the sum rule can be explained by $U/4t_0 \sim 0.7$. From this we derive a correlation energy $U \sim 9$ eV. These values, which demonstrate the importance of electron-electron correlations in $trans$-$(CH)_x$ are in excellent agreement with previous estimates of the correlation energy by Baeriswyl and Maki.[35] On the other hand, our rather large U disagrees with $U = 3$ eV derived from electron nuclear triple resonance spectroscopy[36] and with estimates $U/4t_0 < 0.45$ by Kivelson and Heim.[37]

As shown in Fig. 2, the real part of the dielectric function $\epsilon_1^{\|}$ has a zero crossing with positive slope near 4.6 eV. Since at this energy $\epsilon_2^{\|}$ is small, the π plasmon appears in the loss function nearby at 4.9 eV. This energy position is slightly higher than those given in previous ELS investigations on nonoriented Shirakawa material. For $q = 0.1$ Å^{-1} Ritsko et al.[19] as well as Zscheile et al.[20] observed the π plasmon near 4.2 eV. The lower density of the Shirakawa material compared to that of our polymer leads to a lower $\pi \rightarrow \pi^*$ oscillator strength and thus to a zero crossing of ϵ_1 at lower energies.

Above 5 eV, $\epsilon_2^{\|}$ as well as the $\mathscr{f}^{\|}$ [see Fig. 4(a), $q=0.1$

Å^{-1}] show a series of additional excitations. There is a small peak near 6.6 eV which also appears in the absorption spectra of Baeriswyl et al.[13] The intensity of the peak is changing from sample to sample. The origin of this peak is not clear. Near 8 eV, an increase in $\epsilon_2^{\|}$ is observed. At 12 and 14.6 eV two maxima and near 19 eV a weak shoulder are observed. Within the approximation of noninteracting zig-zag planes, the situation is very similar to that of two-dimensional noninteracting graphite planes.[38] With q in the plane, transitions are allowed only between states of the same parity with respect to a reflection in the plane, i.e., $\pi \rightarrow \pi^*$ and $\sigma \rightarrow \sigma^*$ transitions are allowed. Transitions between states of opposite parity with respect to a reflection in the plane, i.e., $\pi \rightarrow \sigma^*$ transitions, are allowed for q perpendicular to the plane. As there is no macroscopic orientation of the zig-zag planes perpendicular to the chain axis, $\epsilon^\perp$ has contributions from equal and opposite parity transitions whereas $\epsilon^{\|}$ is entirely due to equal transitions. Following these simple selection rules, the 12 eV transition is assigned to a $\sigma \rightarrow \sigma^*$ transition at the Γ point in agreement with the calculations by Mintmire and White[14] (MW). The 14.6 eV transition as well as the 19 eV shoulder must be ascribed to $\sigma \rightarrow \sigma^*$ transitions probably at the boundary of the Brillouin zone.

For momentum transfer perpendicular to the chain axis the imaginary part of the dielectric function in the $\pi \rightarrow \pi^*$ transition range is much lower than that for q parallel to the chain axis. Near 2 eV a strong anisotropy of about 170 is found for ϵ_2. As outlined before, no $\pi \rightarrow \pi^*$ transitions for q perpendicular to the zig-zag plane are allowed. For q in the zig-zag plane, Baeriswyl et al.[13] have calculated $\epsilon_2^\perp$. They obtained a narrow square-root singularity at the gap energy. Above 2 eV, their $\epsilon_2^\perp$ reaches a value of 0.5, for q in the zig-zag plane which results in a value $\epsilon_2^\perp \sim 0.25$ for random orientation perpendicular to the chain axis. This value is in good agreement with $\epsilon_2^\perp \sim 0.2$ in this energy range, derived by the Kramers-Kronig analysis of the loss function. Due to the small weight, the narrow singularity proposed in the calculations is not observed. In addition, the same mechanism discussed for the broadening of the square-root singularity for q parallel to the chain axis will also lead to a broadening for q perpendicular to the chain axis.

At higher energies, $\epsilon_2^\perp$ as well as the $\mathscr{f}^\perp$ (see Fig. 5, $q=0.1$ Å^{-1}) increases above 8 eV. A first maximum appears near 10 eV. According to the calculations of MW (Ref. 4) this peak should occur at 9 eV and is assigned to a $\pi \rightarrow \sigma^*$ transition. A large joint density of states should appear for this transition, as the π and the lowest σ^* band are effectively parallel for a large portion of the Brillouin zone. Additional transitions are observed in $\epsilon_2^\perp$ at 16.5 eV and a broad shoulder near 23 eV. Unfortunately, no calculations of the transition matrix elements at these energies are available. Therefore, an assignment of these transitions which may be $\pi \rightarrow \sigma^*$, $\sigma \rightarrow \pi^*$, or $\sigma \rightarrow \sigma^*$ transitions, is not possible at present.

Only few results on the dielectric functions at higher energies have been obtained by optical spectroscopy. Baeriswyl et al.[13] have measured the optical absorption on oriented Shirakawa material up to 10 eV. They observed no anisotropy in the energy range 5—10 eV which

may be explained by an incomplete alignment of the polymer chains in their samples.[39] Mitani et al.[18] have measured the reflectivity of nonoriented Shirakawa polyacetylene by synchrotron radiation in the energy 1 to 25 eV. Besides the $\pi \rightarrow \pi^*$ transition, the derived ϵ_2 shows a series of excitations at energies above 8 eV.

In the following we discuss the momentum dependence of the dielectric functions of polyacetylene. The π plasmon shows a linear dispersion in momentum transfer in the range $q = 0.05-1.1$ Å^{-1} as can be seen in Figs. 3 and 6. The slope (3.3 eV/Å^{-1}) is slightly smaller than that reported by Ritsko et al.[19] (3.6 eV/Å^{-1}). This result is in line with the prediction of MW (Ref. 14) that material with higher density should exhibit a smaller plasmon dispersion. Above $q = 1$ Å^{-1}, there are deviations from the linear dispersion and a sudden decrease in the intensity appears. Both facts can be explained by damping of the plasmon by interband transitions as will be discussed later in more detail. Below 0.05 Å^{-1} (not shown in Figs. 3 and 6) a sudden decrease in the energy of the π plasmon is observed. For $q=0$, the maximum is observed near 4.3 eV. This deviation from a linear dispersion was already observed in measurements on fibrous Shirakawa trans-polyacetylene by Zscheile et al.[20] Recently, Drechsler and Bobeth[40] have explained this fact by an effective medium approximation for the dielectric function of the polyacetylene fibers. The polyacetylene used in the present investigation had a dense nonfibrous morphology.
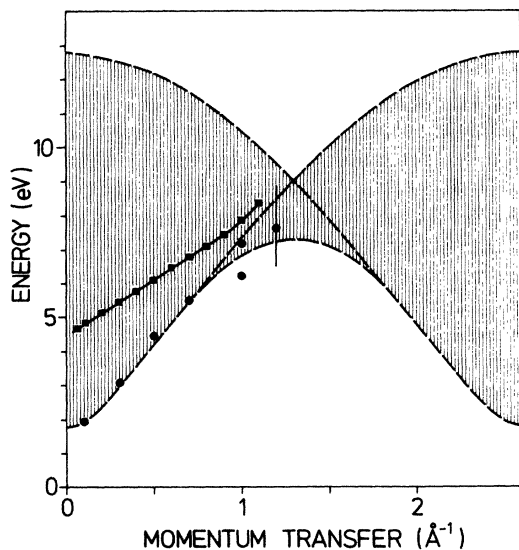

FIG. 6. Possible excitations of π electrons in polyacetylene with momentum transfer parallel to the chain axis. ■: Experimental data on the π plasmon. ●: Maxima of $\pi \rightarrow \pi^*$ interband transitions as derived from the optical joint density of states. Vertical bar indicates a broader distribution of interband transitions. Hatched area indicates the region of possible interband transitions calculated in a tight-binding scheme. Dashed lines show maxima in the calculated joint density of states. If matrix elements were included, transitions near the dashed line starting at $E=12.8$ eV and $q=0$ and ending at 1.8 eV and $q=2.6$ Å^{-1} would be strongly suppressed.

Therefore, another explanation is necessary for the low q dispersion of the π plasmon. It is well known that at small momentum transfer, surface plasmons are excited when electrons are transmitted through thin films.[41] The intensity of surface plasmons decreases with q^{-3}, while that of volume plasmons decreases with q^{-2}. The cross section for surface excitations is proportional[41] to Im$[-1/(\epsilon+1)]$. Thus, the surface π plasmon should appear at $\epsilon_1 = -1$, i.e., at an energy smaller than the volume π plasmon. A calculation of the surface loss function Im$[-1/(\epsilon+1)]$ yields a maximum near 4.2 eV which is close to the observed energy position $E=4.3$ eV. This analysis clearly demonstrates that for small momentum transfer ($q<0.05$ Å^{-1}) the spectra are dominated by surface losses. Therefore, no information on the dispersion of the volume π plasmon in this momentum-transfer range can be obtained from the present measurements.

For the understanding of the momentum dependent $\mathcal{J}^{\parallel}$, we have performed a simple calculation of the joint density of states of the π bands. Similar to previous studies,[17,19] we have calculated the π bands by a simple tight-binding model. In this model the energy bands along the chain are given by

$$E(k) = \pm [\beta_1^2 + \beta_2^2 + 2\beta_1\beta_2\cos(ka)]^{1/2} ,$$

where β_1 and β_2 are the transfer integrals between successive sites, and a is the unit cell length. For the transfer integrals we used $\beta_1 = 3.64$ eV and $\beta_2 = 2.75$ eV. As will be explained later in more detail, this choice gives the best agreement with our experimental data. These values of the transfer integrals correspond to a gap energy $E_g = 2(\beta_1 - \beta_2) = 1.8$ eV and to a total bandwidth between the bottom of the valence band and the top of the conduction band $4t_0 = 2(\beta_1 + \beta_2) = 12.8$ eV. Using a simple sampling procedure,[42] we have calculated the momentum-dependent joint density of states as shown in Fig. 4(b). A broadening of 0.2 eV was included for comparison with the experimental data. For $q=0.1$ Å^{-1}, two singularities at 1.9 eV and at 12.7 eV are realized. Calculations[13,15,16] for the transitions probability between π bands indicate that transitions at the zone center are strongly suppressed, i.e., the singularity at 12 eV is hardly detectable. With increasing momentum transfer the width of the JDOS decreases, in particular, the gap increases linear in momentum transfer for $q>0.1$ Å^{-1}. Above $q=0.8$ Å^{-1} the slope for the lowest singularity decreases and a splitting is observed. The positions of the singularities in the Brillouin zone are shown as a function of momentum transfer in Fig. 6 by broken lines. The same curves are obtained using the analytical RPA expression given by Drechsler and Bobeth[16] as they have used the same band structure for the π-electron system. The hatched area indicates the region of possible $\pi \rightarrow \pi^*$ transitions neglecting matrix element effects. Disregarding the line coming from 12.8 eV at $q=0$ to 1.8 eV at $q=2.6$ Å^{-1} as well as the gap of 1.8 eV, the curves are very similar to those calculated by Williams and Bloch[43] for a one-dimensional metal.

We now compare the theoretical results with our experimental data of the $\mathcal{J}^{\parallel}$ shown in Fig. 4(a). The momentum dependence of the measured maximum of the $\pi \rightarrow \pi^*$

transitions is shown in Fig. 6 by black circles. A strong dispersion of this maximum is observed in good agreement with the theory. The input parameters of the tight-binding calculations (or RPA calculation) were changed in such a way as to reproduce the experimental data. Thus, it was possible to derive the above given parameters $E_g = 1.8$ eV and $4t_0 = 12.8$ eV. These experimental values, in particular the total bandwidth depend, however, on the momentum dependence of the refractive index, which is needed for the Kramers-Kronig analysis. For example, using $n(q)$ calculated for an isotropic semiconductor model[29] yields $4t_0 = 11.5$ eV. However, we think that the latter model is much less adequate for q parallel to the chain axis than the RPA calculation by Drechsler and Bobeth.[16] Therefore, we give for the total bandwidth of the π-electron system the value 12.8 ± 0.5 eV. This value is slightly higher than $4t_0 = 10-12$ eV derived from band-structure calculations by Grant and Batra.[11]

The splitting of the singularity above $q_c = 0.7$ Å^{-1}, predicted by the tight-binding and the RPA calculations, is clearly seen in the OJDS at $q = 1$ Å^{-1}. However, the splitting is considerably larger than that obtained from the calculations. The origin of this discrepancy is not clear at present. At $q = 1.2$ Å^{-1}, the maximum due to the two $\pi \rightarrow \pi^*$ singularities appears slightly broadened. This may be caused by $\sigma \rightarrow \sigma^*$ transitions in the same energy range or by a hybridization of the π bands and the σ bands.

The linear dispersion of the $\pi \rightarrow \pi^*$ interband transitions causes the linear dispersion of the π plasmon. When the $\pi \rightarrow \pi^*$ oscillator moves to higher energies, the zero crossing of $\epsilon_1^{\parallel}$, which leads to the π plasmon, also moves to higher energies. The positions of the π plasmon are indicated by arrows in Fig. 4(a). At low momentum transfer, the π plasmon is in a region of small OJDS, i.e., the plasmon is almost not damped by interband transitions. Above $q = 1$ Å^{-1} the OJDS increases at the energy position of the π plasmon and thus the plasmon is strongly damped by $\pi \rightarrow \pi^*$ transitions. This can be seen more clearly in Fig. 6. Since the slope of the plasmon dispersion is smaller than that of the $\pi \rightarrow \pi^*$ transition, the plasmon curves comes closer to the interband curve at higher momentum transfers. Above $q = 1$ Å^{-1}, the plasmon approaches the region of higher single-particle transition probability. Therefore, the damping of the π plasmon strongly increases. This result for the one-dimensional semiconductor polyacetylene is different from the theoretical calculations by Williams and Bloch[43] for the one-dimensional metal, where no Landau damping is predicted for the free electron plasma.

Figure 4(a) also shows a strong dispersion of the $\sigma \rightarrow \sigma^*$ transitions for q parallel to the chain axis. At present, we cannot analyze this dispersion and the appearance of new maxima in the framework of existing band-structure calculations. Nevertheless, we point out that MW (Ref. 14) have also calculated a decrease of the gap for the $\sigma \rightarrow \sigma^*$ transitions, which is observed in the experimental data shown in Fig. 4(a).

For q perpendicular to the chain axis, no dispersion of the $\pi \rightarrow \sigma^*$ transition at 10 eV in the $\mathscr{f}^{\perp}$ is observed (see Fig. 5) in agreement with the calculations of MW (Ref.

14). Moreover, no dispersion is found for the higher energy transitions (probably $\sigma \rightarrow \sigma^*$ transitions). Going to higher momentum transfer, the changes of the $\mathscr{f}^{\perp}$ for the $\pi \rightarrow \pi^*$ transitions between 2 and 6 eV are small. These results are in line with the concept of a rather small transfer integral perpendicular to the chains.

Up to now, all results could be well explained in a single-particle model. There remains the problem of a strong oscillator strength at higher q between the absorption onset at 1.4 eV for $q = 0$ and the calculated gap which is for $q = 1$ Å^{-1} near 6 eV. The fact that the gap does not increase with increasing momentum transfer was already observed in nonoriented polyacetylene by Ritsko et al.[19] In their investigation, they found for $q > 0.5$ Å^{-1} a dispersionless peak at 2.4 eV which is already present in the loss function and a high oscillator strength in the energy range 1.4–5 eV for $q = 0.7$ Å^{-1} which is comparable with that of the $\pi \rightarrow \pi^*$ transition. The deviation from a single-particle picture was explained in terms of an excitonic enhancement of the absorption edge. However, as they measured on nonoriented samples, it was not possible to exclude that the oscillator strength in consideration was caused by excitations with q transverse to the chain. In our data for the $\mathscr{f}^{\parallel}$, the dispersionless peak at 2.4 eV does not appear. Also in the loss function (see Fig. 3), there is no indication of a shoulder at 2.4 eV at higher momentum transfer. However, we observed an increasing oscillator strength between 1.4 eV and the calculated gap at higher momentum transfer. This intensity is already seen in the momentum dependent loss function as shown in Fig. 3 and is therefore not an artifact of the Kramers-Kronig analysis. An explanation by transitions with q perpendicular to the chain axis can be ruled out as our polyacetylene is almost perfectly oriented. As can be seen from infrared spectroscopy and from electron diffraction, there are no detectable chain segments perpendicular to the orientation axis. The discussed oscillator strength may also be caused by a double-scattering process, namely a combination of an inelastic scattering at $q = 0$ and a quasielastic scattering with the settled momentum transfer. This would give rise to intensity in the measured spectra near the surface π plasmon and the volume π plasmon for $q = 0$ at energies near 4 and 5 eV. Such peaks slowly appear at $q > 1$ Å^{-1} for our sample thickness. To test the influence of this kind of double scattering, we have measured spectra at $q = 1.0$ Å^{-1} for two samples, the thickness of which differ roughly by a factor of 2. Near 5 eV, there is a slight reduction in intensity of the thinner sample. However, for lower energies, the intensity in the loss function remains almost the same. Therefore, the discussed intensity cannot be explained by a double-scattering process. Furthermore, this statement is supported by the lack of a temperature dependence of this intensity as outlined in more detail below. The quasielastic scattering should be strongly temperature dependent. Finally, there may occur phonon-assisted transitions in this energy range. In order to obtain more information on such transitions, we have measured the dielectric functions for $q = 0.7$ Å^{-1} at $T = 80$, 290, and 390 K. Within error bars we did not find any variation of the oscillator strength in the energy range 2–5 eV at $q = 0.7$ Å^{-1} as a

function of temperature. This is a strong indication that the transitions below the calculated gap for higher momentum transfer cannot be explained by interband transitions which are assisted by acoustic phonons. As the energy of the optical phonons is much higher than the energy corresponding to our measuring temperatures, we also can exclude transitions assisted by the absorption of optical phonons. Transitions assisted by the emission of optical phonons cannot be excluded from our experimental data. However, we think we can generally exclude the explanation by phonon-assisted transitions because it is well known from optical spectroscopy on semiconductors that these transitions are about 2 orders of magnitude less intense than the direct transitions.

We also mention that $\pi \rightarrow \sigma^*$ or $\sigma \rightarrow \sigma^*$ transitions cannot explain the oscillator strength below the calculated gap in a tight-binding model, as band-structure calculations[11,12,14] reveal a direct or indirect gap for these transitions of about 5 and 9 eV, respectively.

When we accept all the previous arguments against a simple explanation of the oscillator strength below the calculated gap then the most likely explanation is an excitonic nature of this intensity. There are several theoretical studies on polyacetylene, which point out that there is an excitonic enhancement of the absorption edge[6-10] when electron correlations are taken into account. Unfortunately, there exist, to our knowledge, no calculations on the momentum dependence of excitons in these systems. Thus, no information is available on the wave function and on the transition matrix elements at finite momentum transfer. It is interesting to note that polydiacetylenes which have a very similar π-electron structure and which are also well oriented, show almost the same momentum dependence of the loss function below 8 eV for q parallel to the chain axis.[44] No momentum dependence of the absorption onset and a considerable intensity between the absorption onset and the π plasmon was found. From optical measurements,[45,46] there is some evidence that the fundamental absorption edge is an exciton with a binding energy of 0.5 eV.

For higher momentum transfers, the present investigation reveals an almost linear increase of the oscillator strength between the onset of the absorption edge and the calculated single-particle gap. The total amount of this excitonic oscillator strength is slightly less than the single-particle $\pi \rightarrow \pi^*$ transition intensity. The reason

why we do not see a sharp excitonic line at the absorption onset is not clear at present. A possibility is that increasing intensity of the excitonic oscillator strength may be caused by an excitonic series which joins to the continuum. To fully understand the experimental facts, more theoretical work on the momentum dependence of excitonic transitions in these quasi-one-dimensional systems is necessary.

V. SUMMARY

We have measured the momentum-dependent dielectric functions parallel and perpendicular to the chains of highly oriented polyacetylene in the energy range 0.2–30 eV and in the momentum-transfer range 0.05 to 1.2 $\overset{\circ}{A}{}^{-1}$. Thus information on single-particle and collective excitations of the quasi-one-dimensional Peierls-semiconductor polyacetyelene was obtained. Most of the experimental data could be explained in the framework of a simple tight-binding or a RPA calculation. By a comparison of the theory with the experimental results, a total width of the π band $4t_0 = 12.8 \pm 0.5$ eV could be derived. From an evaluation of the partial sum rule for π-electron excitations, the ratio of the electron-electron correlation energy U to the total width of the π bands $U/4t_0 \sim 0.7$ is estimated. This yields a rather high value for the correlation energy $U \sim 9$ eV which indicates the importance of correlations for the π electrons in $trans$-$(CH)_x$. The measurements give also detailed information on $\pi \rightarrow \sigma^*$ and $\sigma \rightarrow \sigma^*$ excitations and thus on the band structure of the σ electrons.

Most of the results on the dielectric functions can be explained in a single-particle picture. However, in this model a strongly momentum-dependent gap is predicted, which is not observed in the experiments. There, the onset of the absorption is found to be independent of the momentum transfer and considerable oscillator strength appears at higher momentum transfer between this onset and the calculated single-particle gap. The most likely explanation of this oscillation strength is that it is related with transitions which are excitonic in nature.

ACKNOWLEDGMENTS

[1]See, for example, J. C. W. Chien, *Polyacetylene: Chemistry, Physics and Materials Science* (Academic, Orlando, Florida, 1984).

[2]L. G. S. Brooker, Rev. Mod. Phys. **14**, 275 (1982).

[3]H. C. Longuet-Higgins and S. Salem, Proc. R. Soc. London, Ser. A **251**, 172 (1959).

[4]M. Tsuji, S. Huzinaga, and T. Hasino, Rev. Mod. Phys. **32**, 425 (1960).

[5]J.-H. André and G. Leroy, Int. J. Quantum Chem. **5**, 557 (1961).

[6]A. A. Ovchinnikov, I. I. Ukrainskii, and G. V. Kventsel, Usp. Fiz. Nauk **108**, 81 (1972) [Sov. Phys.—Usp. **15**, 575 (1973)].

[7]N. A. Cade, Chem. Phys. Lett. **53**, 45 (1978).

[8]M. Kertész, Chem. Phys. **44**, 349 (1979).

[9]I. I. Ukrainskii, Phys. Status Solidi B **106**, 55 (1981).

[10]D. Pugh, Mol. Phys. **26**, 1297 (1973).

[11]P. M. Grant and I. P. Batra, Synth. Met. **1**, 193 (1979/80); Solid State Commun. **29**, 225 (1979).

[12]J. Ashkenazi, E. Ehrenfreund, Z. Vardeny, and O. Brafman, Mol. Cryst. Liq. Cryst. **117**, 193 (1985).

[13]D. Baeriswyl, G. Harbeke, H. Kiess, E. Maier, and W. Meyer, Physica (Utrecht) **117B**, 617 (1983).

[14]J. W. Mintmire and C. T. White, Phys. Rev. B **27**, 1447 (1983); **28**, 3283 (1983).

[15]T. K. Lee and S. Kivelson, Phys. Rev. B **29**, 6687 (1984).

[16]S. L. Drechsler and M. Bobeth, Phys. Status Solidi B **131**, 267

(1985).

[17]C. R. Fincher, M. Ozaki, M. Tanaka, D. Peebles, L. Lauchlan, and A. J. Heger, Phys. Rev. B **20**, 1589 (1979).

[18]T. Mitani, S. Suga, Y. Tokura, K. Koyama, I. Nakada, and T. Koda, Int. J. Quantum Chem. **18**, 655 (1980).

[19]J. J. Ritsko, E. J. Mele, A. J. Heeger, A. G. MacDiarmid, and M. Ozaki, Phys. Rev. Lett. **44**, 1351 (1980); J. J. Ritsko, Phys. Rev. B **26**, 2192 (1982); J. J. Ritsko, Mat. Sci. **7**, 337 (1981).

[20]H. Zscheile, R. Gründler, U. Dahms, J. Fröhner, and G. Lehmann, Phys. Status Solidi B **121**, K161 (1984).

[21]G. Leising, Polymer Bulletin **11**, 401 (1984).

[22]J. H. Edwards and W. J. Feast, Polymer Commun. **21**, 595 (1980).

[23]J. Fink, Z. Phys. B **61**, 463 (1985).

[24]J. Daniels, C. Festenberg, H. Raether, and K. Zeppenfeld, in *Optical Constants of Solids by Electron Spectroscopy*, Vol. 54 of *Springer Tracts in Modern Physics*, edited by G. Höhler (Springer, New York, 1970), pp. 77.

[25]G. Leising *et al.* (unpublished).

[26]G. Leising, R. Uitz, B. Ankele, W. Ottinger, and F. Stelzer, Mol. Cryst. Liq. Cryst. **117**, 327 (1985).

[27]J. Hubbard, Proc. Phys. Soc. London **58**, 976 (1955).

[28]C. H. Chen and J. Silcox, Phys. Rev. Lett. **35**, 390 (1975).

[29]R. Resta, Phys. Rev. B **16**, 2717 (1977).

[30]W. P. Su, J. R. Schrieffer, and A. J. Heeger, Phys. Rev. B **22**, 2099 (1980); **28**, 1138(E) (1983).

[31]F. Wooten, *Optical Properties of Solids* (Academic, New York, 1972).

[32]P. F. Maldague, Phys. Rev. B **16**, 2437 (1977).

[33]D. Baeriswyl, J. Carmelo, and A. Luther, Phys. Rev. B **33**, 7247 (1986).

[34]D. Baeriswyl (private communication).

[35]D. Baeriswyl and K. Maki, Phys. Rev. B **31**, 6633 (1985).

[36]H. Thomann, L. R. Dalton, M. Grabowski, and T. C. Clarke, Phys. Rev. B **31**, 3141 (1985).

[37]S. Kivelson and D. E. Heim, Phys. Rev. B **26**, 4278 (1982).

[38]F. Bassani and G. Pastori Parravicini, Nuovo Cimento **50**, 95 (1967).

[39]D. Baeriswyl (private communication).

[40]S. L. Drechsler and M. Bobeth, Solid State Commun. **56**, 261 (1985).

[41]H. Raether, in *Excitation of Plasmons and Interband Transitions by Electrons*, Vol. 88 of *Springer Tracts in Modern Physics*, edited by G. Höhler (Springer, Berlin, 1979).

[42]D. Burst, Phys. Rev. **134**, A1337 (1964).

[43]P. F. Williams and A. N. Bloch, Phys. Rev. B **10**, 1097 (1974).

[44]J. J. Ritsko, G. Crecelius, and J. Fink, Phys. Rev. B **27**, 4902 (1983).

[45]Y. Tokura, T. Mitani, and T. Koda, Chem. Phys. Lett. **75**, 324 (1980).

[46]L. Sebastian and G. Weiser, Phys. Rev. Lett. **46**, 1156 (1981).